

Public Reporting burden for this collection of information is estimated to average 1 hour per response, including the time for reviewing instructions, searching existing data sources, gathering and maintaining the data needed, and completing and reviewing the collection of information. Send comment regarding this burden estimate or any other aspect of this collection of information, including suggestions for reducing this burden, to Washington Headquarters Services, Directorate for Information Operations and Reports, 1215 Jefferson Davis Highway, Suite 1204, Arlington, VA 22202-4302, and to the Office of Management and Budget, Paperwork Reduction Project (0704-0188), Washington, DC 20503.

1. AGENCY USE ONLY (Leave Blank)		2. REPORT DATE 31 Jan 08	3. REPORT TYPE AND DATES COVERED 15 Jun 07 - 31 Dec 07	
4. TITLE AND SUBTITLE Reversible Solid Adhesion for Defense Applications			5. FUNDING NUMBERS W911NF-07-1-0348	
6. AUTHOR(S) Dr. Andreas A. Polycarpou				
7. PERFORMING ORGANIZATION NAME(S) AND ADDRESS(ES) University of Illinois at Urbana-Champaign 1901 South First St, Suite A / Champaign IL 61820-7406			8. PERFORMING ORGANIZATION REPORT NUMBER	
9. SPONSORING / MONITORING AGENCY NAME(S) AND ADDRESS(ES) U. S. Army Research Office P.O. Box 12211 Research Triangle Park, NC 27709-2211			10. SPONSORING / MONITORING AGENCY REPORT NUMBER 53029.1-MS-DRP	
11. SUPPLEMENTARY NOTES The views, opinions and/or findings contained in this report are those of the author(s) and should not be construed as an official Department of the Army position, policy or decision, unless so designated by other documentation.				
12 a. DISTRIBUTION / AVAILABILITY STATEMENT Approved for public release; distribution unlimited.			12 b. DISTRIBUTION CODE	
13. ABSTRACT (Maximum 200 words) In this six month project, we have investigated the adhesion behavior between two solid contacting surfaces with the aim of producing both large bond strength, and under conditions of tangential motion weak bond strength, thus achieving reversible adhesion. For this purpose we have used a newly developed dynamic adhesion tester, nominally flat and spherical surfaces ranging in size from micron to millimeter. Based on the experiments, it was found that the faster the velocity in the horizontal (friction) direction, the lower the bond strength, which could be used for debonding. To achieve a strong bond, larger surface areas with a softer material (e.g., gold coating or polymer-based material) should be used. The bond strength also depends on the surface roughness, applied contact force and the presence of humidity. For example, a polymer-based coated sample gave a 167 X reduction in the bond strength under small tangential motions. These results clearly indicate that the bond strength between solid surfaces can be reversed in a controlled manner. This concept can be further advanced for specific military applications and environments and it has the potential to succeed as solid surfaces are very controllable and can be engineered for many different hostile environments.				
14. SUBJECT TERMS reversible adhesion, solid adhesion			15. NUMBER OF PAGES 30	
			16. PRICE CODE	
17. SECURITY CLASSIFICATION OR REPORT UNCLASSIFIED	18. SECURITY CLASSIFICATION ON THIS PAGE UNCLASSIFIED	19. SECURITY CLASSIFICATION OF ABSTRACT UNCLASSIFIED	20. LIMITATION OF ABSTRACT UL	

Reversible Solid Adhesion for Defense Applications

By:

Andreas A. Polycarpou

Department of Mechanical Science and Engineering

University of Illinois at Urbana-Champaign

Submitted for the completion of DARPA Project

Submitted: 01/31/2008

Foreword

It is known that it is usually sufficient to use adhesives to bond two surfaces together. With such adhesives it is difficult, however to get them apart (debond). This work was conducted to investigate how to make two solid surfaces bond firmly and then debond easily, using only the physics of surface interactions and no specialized adhesives.

There has been numerous research works related to adhesion, especially in the areas of microsystems and miniature devices, such as magnetic storage devices and microelectromechanical systems (MEMS). In the cases of microsystems, solid adhesion is typically caused by the smoothness of the approaching/ contacting surfaces and the “cleanliness” of the environment they are in. Adhesion caused by the presence of liquid traces (capillary adhesion) is also common in these applications. Adhesion in these cases is usually catastrophic as it causes surfaces to get stuck and thus rendering the device non functional. With an extensive experience of the principal investigator in modeling and experimental research on solid adhesion, including roughness effects and the presence of thin films at the interface, a different (compared to standard adhesives) approach to reversible adhesion has been investigated in this research [1-7].

Based on the literature and our experience with solid surface adhesion, it is proposed to use controlled solid surfaces to obtain a sufficiently strong bond between two surfaces and also techniques to reverse the effects of adhesion and debond the surfaces within short time duration of milliseconds range. Such reversible adhesion effects would be beneficial to defense applications. For example one could envision remotely sending an object to a target, attaching itself to the target (via strong solid adhesion), for surveying or other purposes, and then after completing its task or if detected, debond itself (via reversible adhesion) and return safely to its destination. In practical cases such reversible adhesion will need to apply to many different types of target surfaces, e.g. buildings, ships, airplanes, etc, which inherently have different surfaces properties and different environments (e.g. operating in air vs. water).

During the six months period of performance of this research, we experimentally investigated and verified the concept of solid adhesion (bonding) and debonding using controlled micron to millimeter size surfaces including surface roughness effects.

Table of Contents

Foreword	1
Table of Contents	2
1. Introduction.....	3
2. Experimental Setup for Dynamic Interfacial Adhesion Force Measurements	4
3. Preliminary Adhesion Experiments	5
4. Adhesion Experiments.....	7
4.1 Test Conditions.....	8
4.2 Sample Preparation	9
5. Experimental Results.....	10
5.1 Horizontal Dynamics of 1 mm x 1 mm Silicon on Silicon	10
5.2 Horizontal Dynamics of 1.6 mm Diameter Steel Sphere on Pressure Sensitive Adhesive Surface.....	11
5.3 Horizontal Dynamics of 1.6 mm Diameter Steel Sphere on Photoresist Coated on Silicon Surface	12
5.4 Horizontal Dynamics of 200 μm x 200 μm Au Coated Silicon on Au Coated Silicon	14
5.5 Horizontal Dynamics of 1 mm x 1 mm Au Coated Silicon on Au Coated Silicon	14
6. Conclusions.....	15
Acknowledgment.....	16
References.....	16
Appendix-Power point slides of the final project presentation presented to Dr. Todd Hylton, Jan 14, 2008.....	16

1. Introduction

In the adhesion, contact mechanics and tribology research communities it has been known for at least half a century that solid adhesion plays a critical role at solid (metallic and other) interfaces, usually resulting in local asperities within an interface adhering to each other with the possibility of the interface “interlocking.” The beginning of this concept goes back to Bowden and Tabor [8], which showed that a clean steel or brass rod pressed on a soft material, such as indium, can cause the two metals to adhere (bond), as shown schematically in Fig. 1. Experiments in ultra high vacuum between metals (where no oxides are present) result in very high friction due to strong adhesion between bare metals. The fact that in everyday surface contacts and tribological applications, friction is relatively low is because of the presence of oxides and contaminants on the surfaces (such as lubricants). In classical (macro) applications, adhesive friction and adhesive wear are considered precursors to catastrophic failures as they result in very high friction and material removal because of the two surfaces adhering to each other. These problems are typically avoided with the presence of lubricants, hard protective coatings and the selection of “appropriate” materials.

In micro applications such as magnetic storage hard disk drives and MEMS, capillary adhesion and solid surface adhesion are very important and have been studied extensively in recent years. Such micro applications involve (a) large surface-to-volume ratios, (b) low loads, (c) surface roughness that are two-to-three orders of magnitude lower (in the nanometer range) than in conventional applications and (d) cleaner (less contaminated) surfaces. In these applications research has focused on understanding and controlling such adhesive interactions via (for example) geometrical changes (contacting surface area and surface roughness) or via chemical modification to the surfaces (e.g., using molecularly thin lubricants). It is exactly this effect that we explored in this research. Building on our analytical and experimental work on solid adhesion, we explored this basic solid surface adhesion phenomenon.

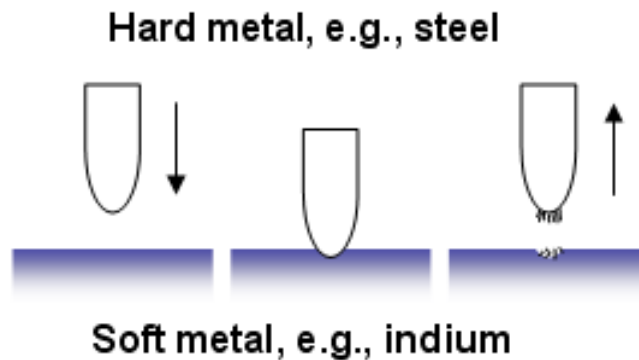


Fig. 1 Schematic showing principle of solid surface adhesion [8].

2. Experimental Setup for Dynamic Interfacial Adhesion Force Measurements

Adhesion (and friction) forces for micro and nanoscale contact systems are typically measured using cantilever type instruments along with optical tools (AFM), as well as surface force apparatus (SFA), e.g., [9]. However, depending upon the material and contact conditions, the cantilever type instruments and the compliant SFAs are difficult to calibrate, and not capable of performing high dynamic bandwidth measurements. For these reasons, a novel instrument has been developed to measure the dynamic interfacial forces directly from a custom-build high dynamic bandwidth force transducer that is placed in line with the approaching and contacting surfaces, as shown in Fig. 2. The uniqueness of this instrument is that in addition to nanometer positioning accuracy it also uses a high dynamic bandwidth force transducer, with the specifications listed in Table 1.

Three different custom-made force transducers were used in this work, as listed in Table 1 to cover the full range of the interfacial forces, with the third transducer being the most sensitive. Referring to Fig. 2(a), using the two closed-loop piezoelectric (PZT) actuators, the vertical and horizontal velocities of the approaching/retracting contacting surfaces can be independently controlled. The displacement resolution of the vertical PZT actuator is 0.6 nm, and the total travel distance is 30 μm . Alignment of the approaching surfaces is ensured using a 3 degrees-of-freedom tilting stage, and a microscope. The interfacial forces are measured using the prototype custom-made capacity-type force transducer which is attached directly on the upper PZT actuator. In order to isolate possible external vibrations, the main holder is attached on a magnetic base which has a resonant frequency of 4.6 kHz. Thus, vibrations due to the two actuators or any other external source do not resonate the holder, unless the frequency component is larger than 4.6 kHz, which is not in all experiments performed in this research. The details of the dynamic adhesion tester and preliminary experiments can be found in [11].

Table 1. Specifications of three different custom-made force transducers.

Transducer ID	Force Constant	Displacement Constant	Spring Constant	Mass
I	0.22 V/gram	0.48 V/ μm	21312 N/m	58 mg
II	2.28 V/gram	0.61 V/ μm	2634 N/m	24.3 mg
III	5.66 V/gram	3.31 V/ μm	5740 N/m	33.3 mg

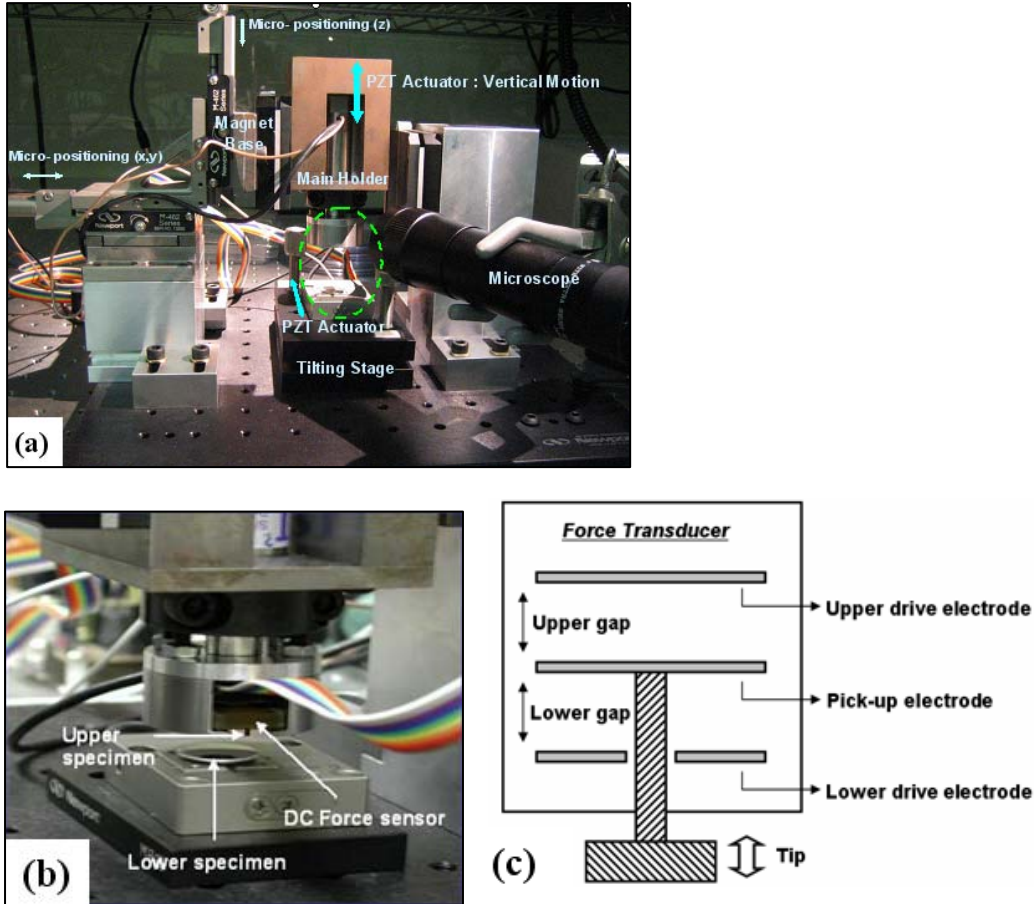


Fig. 2 *Prototype dynamic adhesion tester: (a) overall view, (b) close up of the interface, (c) schematic custom-made dynamic (with DC) capacitive force transducer.*

3. Preliminary Adhesion Experiments

When two surfaces are brought sufficiently close to each other, they may snap-to-contact when they are at a certain distance apart due to the presence of attractive intermolecular (adhesive) forces, such as van der Waals forces. This force is known as pull-in force. Once the surfaces are in adhesive (interlocking) contact, any applied surface displacement in the normal direction gives rise to contact and adhesive forces. Under normal conditions (and the absence of tangential motions/vibrations), when the two surfaces are pulled apart, a certain magnitude of force is needed to separate the contacting surfaces, which is called pull-off force. This force is the strength of the bond (bond strength). Fig 3(a) depicts a representative force displacement curve measured using the dynamic adhesion tester, shown in Fig. 2. The pull-in and pull-off force are affected by the following parameters:

- A. Physical/Geometrical properties
 - Surface roughness
 - Surface energy
 - Hardness and elastic modulus
 - Nominal contact area

B. Interface conditions

- Dry contact
- Humid contact
- Lubricated contact

C. Contact system dynamics

- Approaching velocity
- Retracting velocity
- Tangential velocity

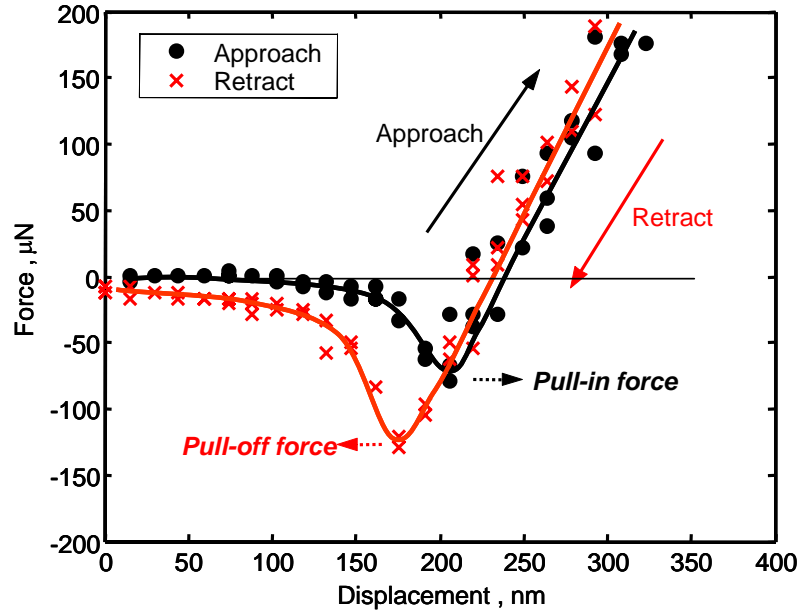


Fig. 3 Representative force-displacement curve obtained from the dynamic adhesion tester.

Using the developed instrument, the dynamic adhesive force between an Al_2O_3 -Tic sphere (1 mm radius) and a very smooth 10 nm thick carbon film disk was measured. The carbon film disk was stationary on the lower PZT actuator, while the Al_2O_3 -Tic sphere was on the upper PZT actuator and was approaching/retracting (in the vertical direction) at constant velocities from 0.074 $\mu\text{m/s}$ to 5.922 $\mu\text{m/s}$. For a given vertical velocity, the adhesive force was measured at three different contact force levels of 70 μN , 220 μN , and 770 μN .

Fig. 4 (a) shows the measured pull-in forces with respect to the vertical velocity. It was observed that the slower approaching velocity gave higher pull-in force. As expected, the pull-in force did not show any dependency on the contact force level, as it is determined by the non-contact intermolecular interactions. Fig. 4 (b) shows the measured pull-off force (debond strength) with respect to the vertical retracting velocity. As in the pull-in force measurements, it was found that lower retracting velocity gave higher pull-off forces. However, contrary to the pull-in force measurements, the pull-off force showed clear dependence on the contact force level, with higher contact force showing higher pull-off force. This could be caused by the larger real contact area with higher contact forces.

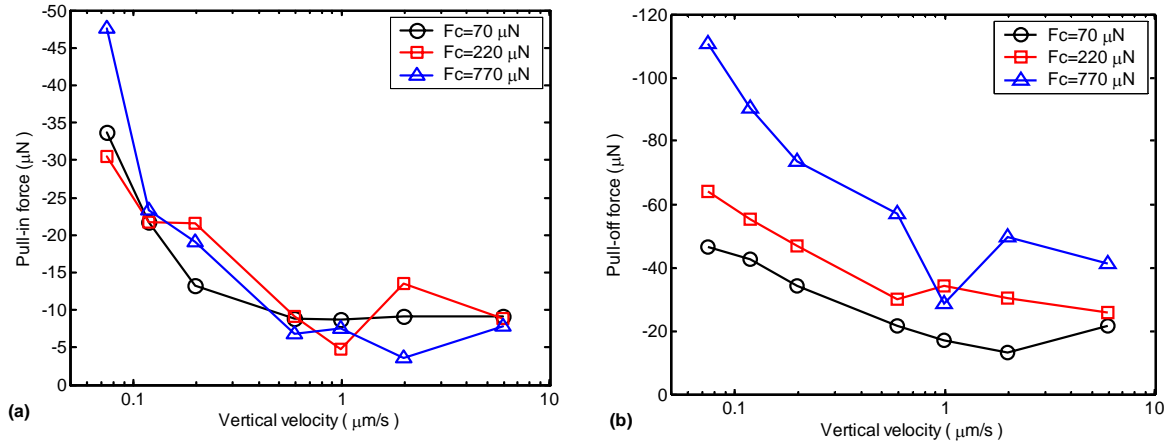


Fig. 4 Dynamic adhesive force measurements between Al_2O_3 -TiC spherical sample and carbon film disk under stationary tangential dynamics.

4. Adhesion Experiments

Depending upon the interface contact conditions, there are several methods to control the adhesive forces (pull-in and pull-off) between rough surfaces in contact. If the two surfaces come into contact using polymer-type surfaces, liquid adhesives, or humidity (water), the pull-off force (bond strength) could be significantly larger and could also be strongly affected by the normal and tangential surface dynamics. For example, when considerable water molecules (high humidity) are between the contacting surfaces, the adhesive force is mainly determined by the meniscus (water bridges between surface asperities). In such cases, if the liquid bridges can be broken by controlling the surface dynamics, e.g. by applying a small amplitude vibration in the lateral (friction) direction, the pull-off force (bond strength) will be very small, thus achieving reversible adhesion and debonding. This is shown schematically in Fig. 5(a)-(b). Note that this principle has been used in contact-start-stop type hard disk drives [10], where during start-up, a high acceleration “jerk” is applied to initiate sliding of the contacting sliders that are strongly adhered to the disks due to, for example, high humidity capillary (meniscus) forces.

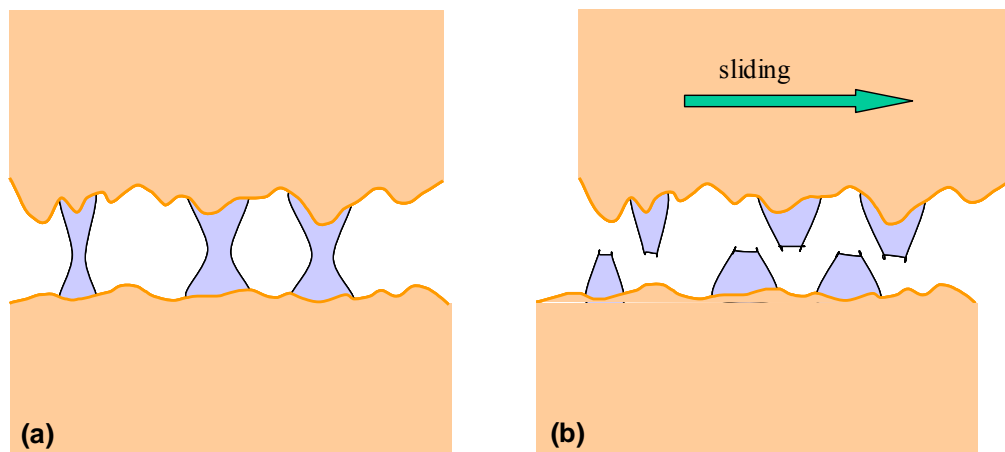


Fig. 5 Schematics showing (a) the formation of liquid meniscus bridges (high bond strength), (b) breaking of the meniscus bridges (debonding) using tangential surface dynamics.

4.1 Test Conditions

In this research, we specifically investigated bonding and debonding of various interface contact conditions. The schematic of Fig. 6(a) and (b) depicts such measurements under (a) dynamic approaching/retracting (normal) conditions and stationary tangential and (b) both dynamic normal and tangential conditions.

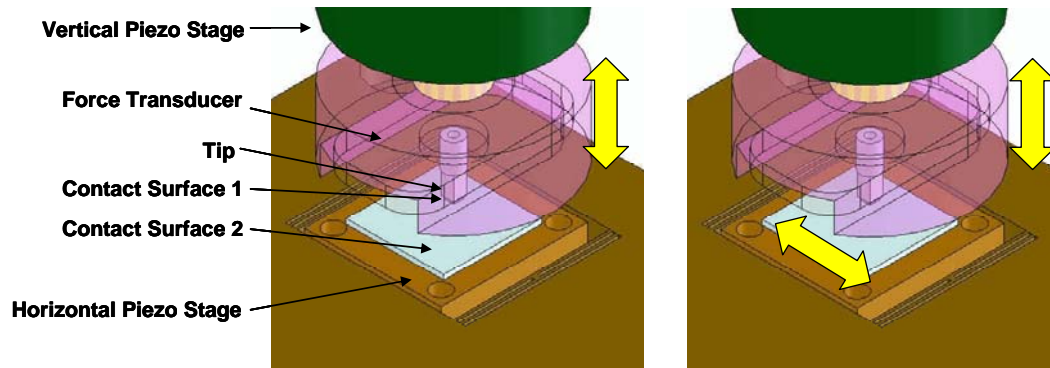


Fig. 6 Schematics showing (a) dynamic normal and stationary horizontal dynamics and (b) both dynamic normal and tangential dynamics.

Fig. 7 shows the displacement profiles of the PZT stages where the upper sample (contact surface 1) provides the vertical movement (VPZT) and the bottom sample (contact surface 2) the horizontal motion (HPZT). The sample on the bottom surface is attached directly on the PZT stage which provides the horizontal movement. The upper sample is attached directly on the custom-made transducer, where the force data is directly measured. The upper sample and transducer are again directly connected to the upper PZT stage which provides the dynamic vertical motion.

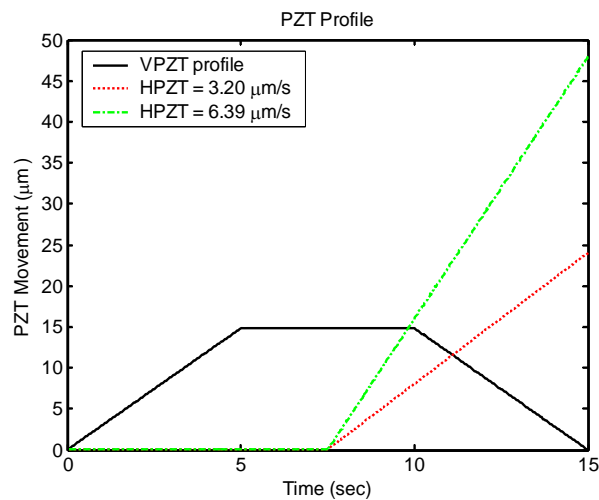


Fig. 7 Displacement profiles of PZT stages (VPZT stands for vertical PZT and HPZT for horizontal PZT).

The solid line (trapezoidal profile) depicts the motion of the upper stage (normal direction). The upper sample moves towards the stationary bottom sample and makes contact, whereas the bottom surface initiates a horizontal movement 2.5 seconds after contact is made. For the first five seconds of the experiment (ramp profile), the upper sample is approaching the bottom surface and makes contact. During the following five seconds, the two surfaces remain in contact and during the last five seconds, the upper sample retracts from the bottom sample (negative slope ramp). The horizontal stage whose motion is shown with the dotted/dashed lines is fully stationary for the first 7.5 seconds of the experiment maintaining interfacial contact and then moves with velocities ranging from 0 $\mu\text{m/s}$ to 4 $\mu\text{m/s}$ for each test case.

A horizontal movement with zero velocity implies that the upper sample makes contact with the bottom surface followed by no-shear force retraction while the horizontal stage remains stationary. The horizontal motion results in a shearing force between the two contacting surfaces, playing a role in breaking the junctions (and meniscus bridges) at the asperity level, formed between the two surfaces.

4.2 Sample Preparation

Different samples were prepared and tested to measure their interfacial pull-off forces (bonding and debonding strengths). The “main” sample is a silicon wafer (orientation $\langle 100 \rangle$), which has a very smooth surface. The main reason for using silicon at this early stage of the research is that silicon has sub nanometer roughness, thus potentially causing high interfacial adhesion, as well as it is the material of choice in microsystems. Also, a spherical ceramic $\text{Al}_2\text{O}_3\text{-TiC}$ sample, a spherical steel sample, a thin film gold coating on silicon sample and a 10 nm thick carbon coated on glass substrate were utilized in this research. All samples were first rinsed in acetone, then in isopropyl alcohol, and then air dried, before testing. The surface roughness measurements of these samples were measured using an atomic force microscope and typical measurements are shown in Fig. 8. The extracted surface roughness parameters (ranging from sub nanometer to tens of nanometers) are listed in Table 2.

Table 2 Test Samples and RMS roughness values

Sample	RMS roughness
<u>Spherical Samples</u>	
Al ₂ O ₃ TiC ball	25.8 nm
Steel ball	5.25 nm
<u>Nominally Flat Samples</u>	
Silicon Wafer	0.11 nm
10 nm Carbon film on Glass	0.77 nm
1 μm Au sputtered on Silicon	3.84 nm

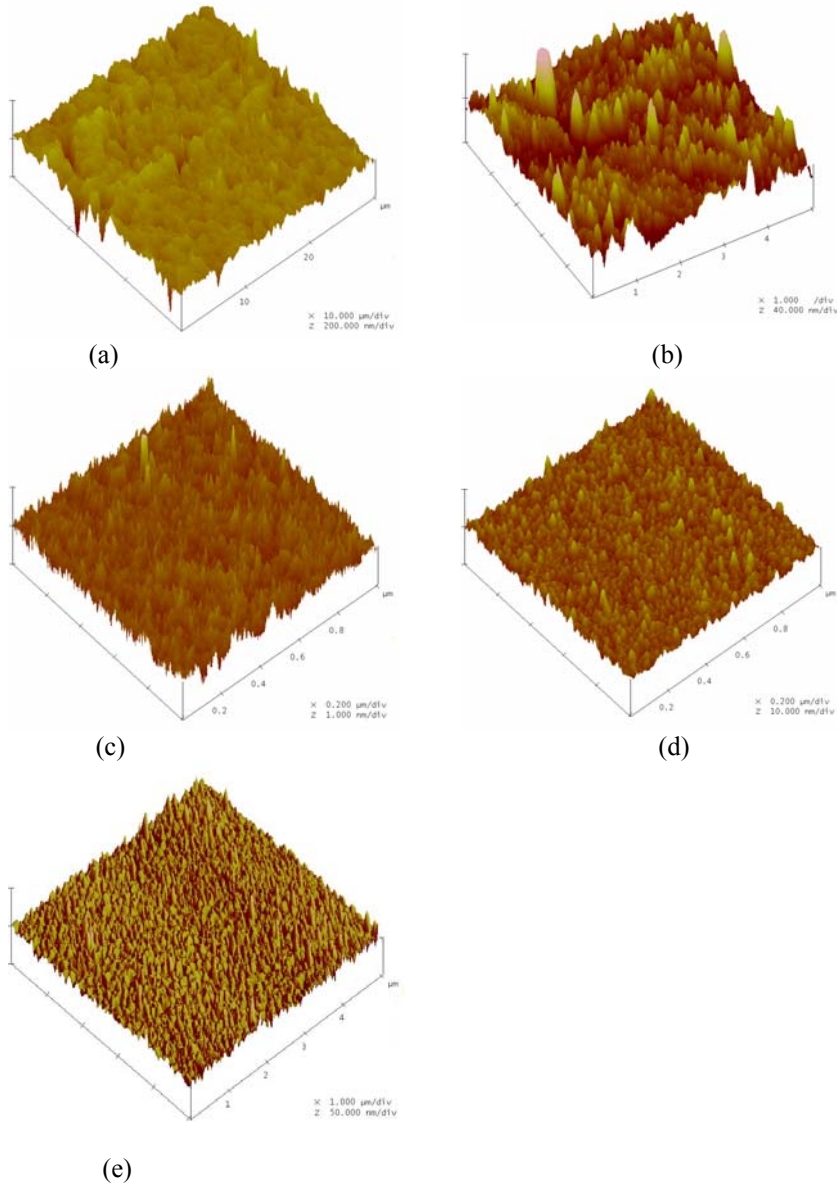


Fig. 8 AFM images of test samples (a) $\text{Al}_2\text{O}_3\text{-TiC}$ sphere, (b) stainless steel sphere, (c) silicon wafer $\langle 100 \rangle$ orientation, (d) 10 nm carbon film on glass substrate and (e) 1 μm thick Au sputtered film on silicon wafer.

5. Experimental Results

5.1 Horizontal Dynamics of 1 mm x 1 mm Silicon on Silicon

Using such mm-size “large” nominally flat samples, the measured pull-off forces (bond strength) are depicted in Fig. 9. The calculated contact pressure (assuming a nominal contact area of 1 mm^2) is 3 kPa for a silicon surface and 3000 μN contact force. However the real contact pressure is expected to be higher as the real contact area is much smaller (due to roughness and possibly minute misalignment of the samples during testing).

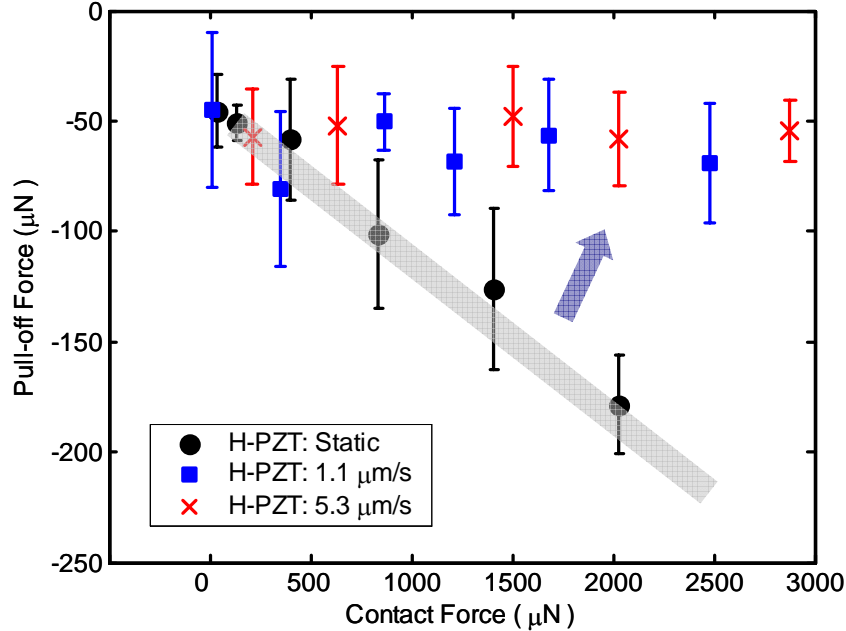


Fig. 9 Pull-off force vs. contact force for 1mm² silicon on silicon samples under stationary and dynamic horizontal velocities.

The horizontal PZT stage begins its movement during midway of the contact process, as described in Sec. 4.1. When the bottom sample is stationary, larger contact forces significantly increase the pull-off force (bond strength). For example, at a contact force of 2000 μN and stationary sample (zero horizontal velocity) the bond strength or pull-off force is -180 μN , where it reduces to -55 μN when the bottom sample is moving horizontally at 5.3 $\mu\text{m/s}$. Note that in these experiments, the pull-off force was almost independent of the horizontal stage's velocity. This implies that the adhesion force rapidly decreases with shearing force even though the normal contact force is as high as 2000 μN .

5.2 Horizontal Dynamics of 1.6 mm Diameter Steel Sphere on Pressure Sensitive Adhesive Surface

Fig. 10 depicts the changes of the pull-off forces when a 1.6 mm diameter steel sphere and a pressure sensitive adhesive (PSA) come into contact with each other. In this case of the spherical sample misalignment issues as with flat-on-flat samples are eliminated. PSA is characterized as being normally tacky and exhibiting instant tack when applied to a substrate. PSA is usually used for storing small samples like AFM tips. A variety of polymers have been used to manufacture PSA, such as acrylic, copolymers, butyl rubber-based systems, silicones, urethanes, vinyl esters, etc. A silicone-based rubber-like PSA having a 330 μm thickness is used in this research.

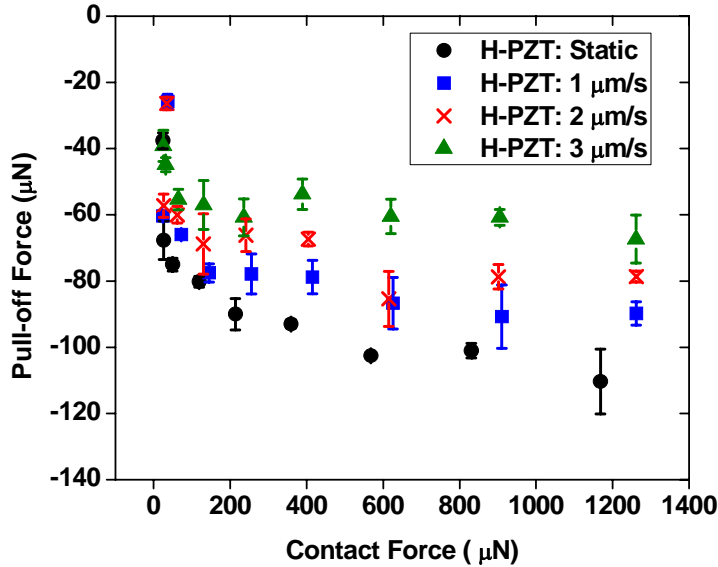


Fig. 10 Pull-off force vs. contact force for 1.6 mm diameter steel sphere on pressure sensitive adhesive under stationary and dynamic horizontal velocities.

Examining the results depicted in Fig. 10, it is clearly seen that the trends are similar to the silicon-on-silicon flat surfaces. That is a decrease in the bond strength with tangential dynamic motions, especially at higher contact forces. Moreover, faster horizontal motion gives lower pull-off forces (thus lower debonding strength). It is also seen that PSA has a significantly lower spread in the data (lower standard deviation) compared to solid-on-solid silicon surfaces. This is most likely due to the masking or averaging effect of the soft PSA, thus reducing the effect of surface roughness. Thus, these surfaces stably contact each other due to the soft characteristics of the PSA surface. Such characteristic of a soft surface can result in obtaining stable interfacial contact behavior. However, under the conditions investigated in this preliminary research it did not exhibit sufficiently large bonding strength and further work is needed. Moreover, the intrinsic sticky characteristics of PSA cause a limit as to how much the bond strength could decrease under a limited range of horizontal motions (vibrations). For applications where the bond strength needs to be in the MPa range, further understanding and optimization of a softer/harder interface is required.

5.3 Horizontal Dynamics of 1.6 mm Diameter Steel Sphere on Photoresist Coated on Silicon Surface

Fig. 11 depicts the experiment results of contacting a photoresist (PR) coated surface on silicon substrate and a 1.6 mm diameter steel sphere. The PR has the trade name of AZ4620 and is manufactured by Clariant. The PR coated sample surface was prepared using a spin coating process for an 8 µm film thickness. Then the PR sample was baked at 60 °C for 1 minute and cured for 2 hours at room temperature (i.e., producing a

not-fully cured sample). By using this not fully cured PR sample, we were able to produce a surface which is softer than the regular fully cured PR.

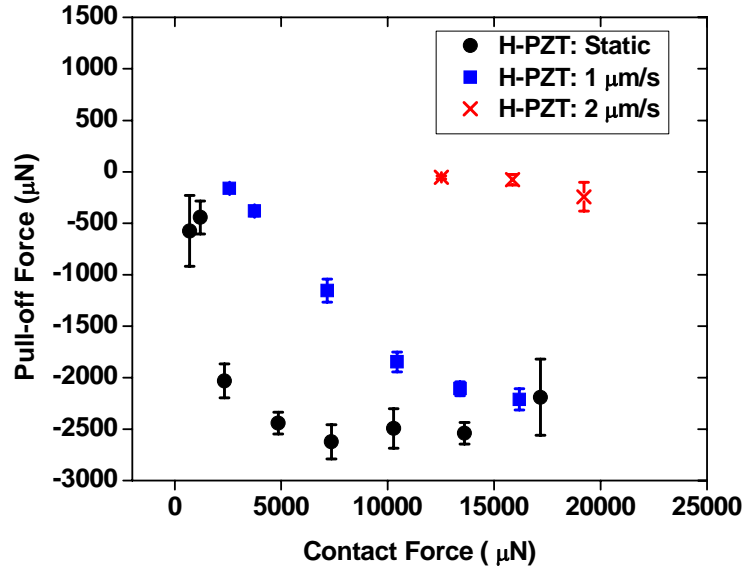


Fig. 11 Pull-off force vs. contact force for 1.6 mm diameter steel sphere and photoresist coated on silicon surface for stationary and dynamic horizontal velocities.

PR, which tends to be “sticky,” was coated to a thin film, thus resulting in a higher range of contact pressures than the case of the PSA sample discussed above. The contact pressure ranges from 28.74 MPa to 54.37 MPa when a steel sphere of 1.6 mm in diameter makes contact with the silicon wafer coated with PR under a force of 13000 µN. These values were obtained using simple layered FEM calculations (ABAQUS). Note that the modulus of elasticity for PR varies from 1 GPa to 4 GPa for PR that has not been fully cured (thus the range in the contact pressures, and thus the bonding strength).

Examining Fig. 11, it is clearly seen that the effect of the tangential velocity has a significant effect on the bond strength, with the pull-off force decreasing with increasing velocity. *At a contact force of 13000 µN and stationary horizontal conditions, the pull-off force was measured to be 2500 µN (bond strength), whereas when the horizontal velocity was 2 µm/s, the pull-off force decreased significantly to only 15 µN (debond strength), which corresponds to over 2 orders of magnitude reduction (to be exact 167 X reduction). This clearly shows that when a hard surface is coated with a polymeric-type surface, higher adhesion forces (and correspondingly higher bond strengths in the MPa range) could be achieved. By applying a controlled horizontal movement (vibration), a significant reduction (of the order of more than two orders of magnitude) in the adhesion force could be realized (corresponding to debonding). This clearly demonstrates the reversible nature of solid adhesion.*

5.4. Horizontal Dynamics of 200 μm x 200 μm Au Coated Silicon on Au Coated Silicon

For these experiments standard photolithographic microfabrication was utilized to fabricate silicon “pillars” of precisely known contact areas. Bare silicon was coated with PR through a spin coating process and then exposed to UV light using a square typed mask before being fabricated through inductively coupled plasma (ICP) etching process. Subsequently these pillars were coated with a gold coating.

Fig. 12 depicts the test results for these experiments. Note that in these experiments the humidity level was also controlled. Specifically two humidity levels were examined, 55% and 30% representing high and low relative humidity, respectively. The calculated contact pressure for these experiments, using the nominal contact area ranges from 12.5 kPa to 75 kPa (for a silicon surface with an area of 200 μm x 200 μm and a contact force that varies from 500 μN to 3000 μN).

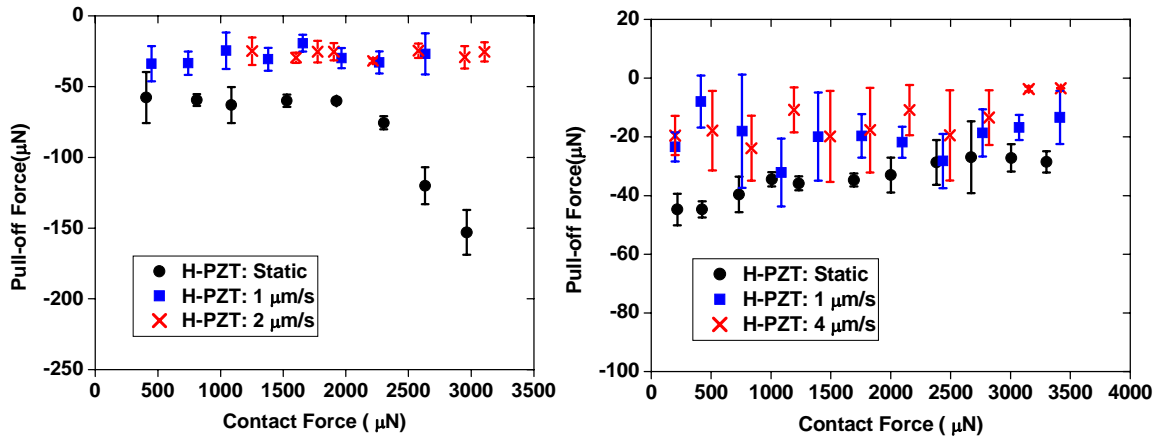


Fig. 12 Pull-off force vs. contact force for 200 μm x 200 μm Au coated silicon on Au coated silicon (a) 55% relative humidity (b) 30% relative humidity.

The overall trends are similar with the previous tests, even though in the current experiments the pull-off force levels are lower due to the smaller contact areas involved. The pull-off force decreased when the horizontal stage moved horizontally compared to the stationary case. As expected, the higher humidity level caused a larger pull off force, under stationary conditions, compared to the lower humidity level. This indicates that the increased humidity level drastically increases adhesion.

5.5. Horizontal Dynamics of 1 mm x 1 mm Au Coated Silicon on Au Coated Silicon

The last set of experiments, shown in Fig. 13, was performed using significantly larger nominal contact areas of gold coated silicon samples. It is clearly seen that the gold coated surfaces have a significantly higher reduction in the bond strength under horizontal motion, compared to the much harder bare silicon surfaces (of the same nominal contact area). At a contact force of 3450 μN , the difference in the pull-off forces for the stationary case (0 $\mu\text{m}/\text{s}$ horizontal motion) and the horizontal dynamic case of 1 $\mu\text{m}/\text{s}$ is 24.2

X larger. Note that unlike the polymer-based surfaces, a lower horizontal velocity results in significant reduction of the bond strength.

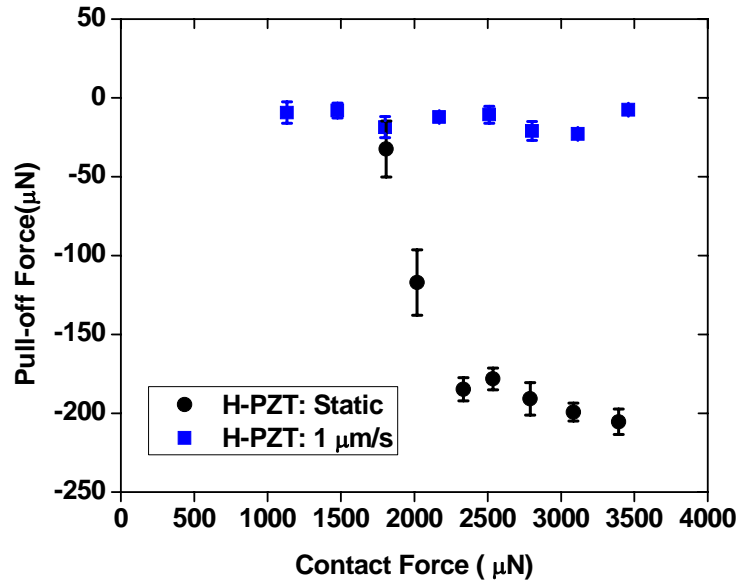


Fig. 13 Pull-off force vs. contact force for 1 mm x 1 mm Au coated silicon on Au coated silicon samples.

6. Conclusions

In this short six month project, we have investigated the adhesion behavior between two solid contacting surfaces with the aim of producing both high bond strength and under conditions of tangential motion produce very weak bond strength, thus achieving reversible adhesion. For this purpose we have used a newly developed specialized dynamic adhesion tester, nominally flat and spherical surfaces ranging in size from micron to millimeter.

The first set of experiments was under conditions of one of the samples (lower sample) being stationary while the upper sample was dynamically loaded and unloaded to the surface (under different approaching velocities). It was found that higher contact forces give larger pull-off forces (higher bond strength) and slower approaching velocities cause earlier jump-in behavior with larger pull-in force. Also, slower retracting velocities cause later jump-out behavior with larger pull-off force.

The second and main phase of experiments were conducted under both dynamic normal and horizontal (in the friction direction) motions. Moreover, both spherical and nominally flat samples were tested, including humidity effects. Based on these experiments, it was found that the faster the velocity in the friction direction, the lower the bond strength, which could be used for debonding. On the contrary, to achieve a strong bond, larger surface areas with a softer material (e.g., gold coating or polymer-based material) should be used. Moreover, the bond strength is dependent on the surface roughness, applied contact force and the presence of humidity. According to Bowden and Tabor [8], solid surface adhesion comes from the

interlocking of the surface asperities. When the applied load is directed perpendicularly to the contacting surfaces, the two surfaces hold together because of adhesion. Such junctions are more easily formed when there is water or other traces of liquids. When there is moisture, adhesion produced in such atmospheres is drastically increased. However, adhesion is drastically reduced by shearing the asperity junctions.

Adhesion also depends on the mechanical properties of the contacting surfaces. This was confirmed by using bare silicon samples with gold coated samples. When the gold coated samples were used, an increase in the adhesion force was measured, compared to the silicon samples. Gold coated samples with the largest (tested in this research) nominal area of 1 mm² under a contact force of 3000 μN, produced a bond strength that was 24.2 times greater under stationary versus dynamic conditions. A polymer-based coated sample gave a much larger ratio of 167 X reduction in the bond strength under small tangential motions. These results clearly indicate that the bond strength between solid surfaces can be readily reversed in a controlled manner.

This preliminary research provides a clear proof-of-concept that using appropriate materials and interface conditions, bond strength can be maximized (strong bond) as well as it can be minimized (weak bond necessary for debonding), thus achieving reversible adhesion with solid surfaces. This concept can be further advanced for specific military applications and environments and it has the potential to succeed as solid surfaces are very controllable and can be engineered for many different hostile environments.

Acknowledgment

This work was sponsored by Defense Advanced Research Project Agency (DARPA) under contract number W911NF-07-1-0348 under the directions of Dr. Don Leo and Dr. Todd Hylton.

References

- [1] Suh, A. Y., and A.A. Polycarpou, "Adhesion and Pull-off Forces for Polysilicon MEMS Surfaces using the Sub-Boundary Lubrication Model," ASME J. of Tribology, **125**, 193-199, 2003.
- [2] Lee, S.-C., and A.A. Polycarpou, "Adhesion Forces for Sub-10nm Flying-Height Magnetic Storage Head Disk Interfaces," ASME J. of Tribology, **126**, 334-341, 2004.
- [3] Suh, A.Y., S.C. Lee, and A. A. Polycarpou, "Adhesion and Friction Evaluation of Textured Slider Surfaces in Ultra-low Flying Head-Disk Interfaces," Tribology Letters, **17:4**, 739-749, 2004.
- [4] Yu, N., W.A. Bonin, and A. A. Polycarpou, "High-resolution Capacitive Load-displacement Transducer and Its Application in Nanoindentation and Adhesion force Measurements," Rev. of Sci. Instr., **76:4**, Article No. 045109, 2005.
- [5] Shi, X., and A. A. Polycarpou, "An Elastic-plastic Hybrid Adhesion Model for Contacting Rough Surfaces in the Presence of Molecularly Thin Lubricant," J. Colloid and Interf. Sci., **290:2**, 514-525, 2005.
- [6] Tayebi, N., and A. A. Polycarpou, "Reducing the Effects of Adhesion and Friction in Microelectromechanical Systems (MEMS) through Surface Roughening: Comparison Between Theory and Experiments," J. of Applied Physics, **98:7**, Art. No. 073528, Oct. 2005.

- [7] Xue, X., and A.A. Polycarpou, "An Improved Meniscus Surface Model for Contacting Rough Surfaces," *J. of Colloid and Interf. Sci.*, **311**, 203-211, 2007.
- [8] Bowden, F.P., and D. Tabor, *An Introduction to Tribology*; Anchor Press/Doubleday, 1973
- [9] Benz, M., K.J., Rosenberg, E.J. Kramer, and J.N. Israelachvili, "The Deformation and Adhesion of Randomly Rough and Patterned Surfaces," *J. Phys. Chem. B*, **110**, 11884-11893, 2006.
- [10] Li, Y., and A. K. Menon, "A Theoretical analysis of breakaway friction measurement," *ASME J. of Tribology*, **116**, 280-286, 1994.
- [11] Yeo, C.-D., S.-C. Lee, and A.A. Polycarpou, "Dynamic Adhesive Force Measurements under Vertical and Horizontal Motions of Interacting Rough Surfaces," *Rev. of Sci. Instr.*, **79**, Art. No 015111, 2008.

Appendix- Power point slides of the final project presentation as presented to Dr. Todd Hylton, Jan 14, 2008

Reversible Solid Adhesion for Defense

Applications: W911NF-07-1-0348

Final Report Presentation: January 14, 2008
Period of Performance: 15 June 2007 - 31 December 2007
ARO Grants Officer: Dr. David M. Stepp

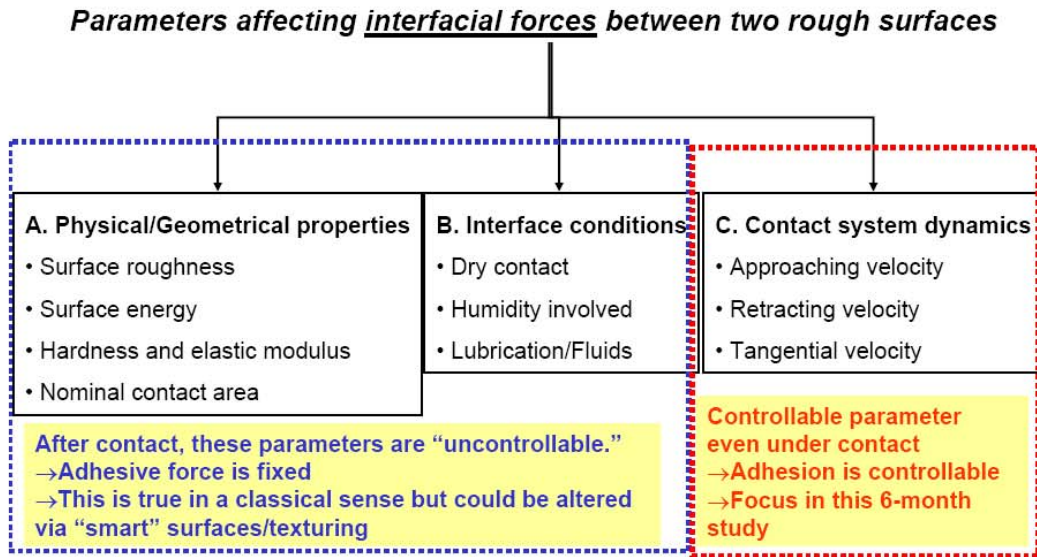
Submitted to: Dr. Todd Hylton, DARPA Program Manager
PI: Andreas A. Polycarpou
PhD Students: Jungkyu Lee and Chang-Dong Yeo

Department of Mechanical Science and Engineering
University of Illinois at Urbana-Champaign

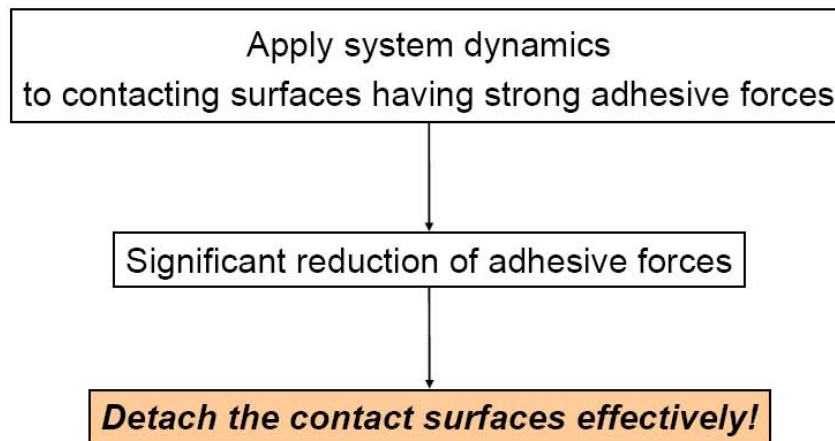
Outline

1. Motivation
2. Project Goal
3. Significant Results-Executive Summary
4. Instrumentation
5. Sample Preparation
6. Experimental Results
7. Summary

1. Motivation



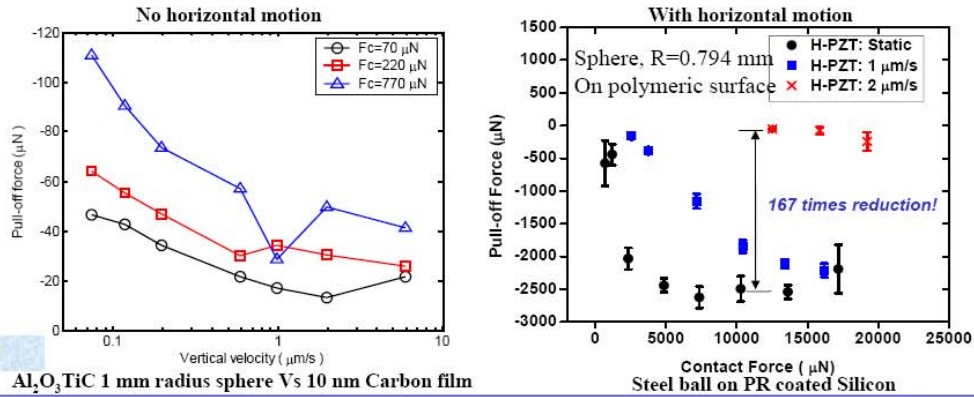
2. Project Goal



→ Demonstrate strong bond and weak debond strengths

3. Significant Results-Executive Summary

- Pull-off force measurements, vertical dynamics: **High Bond Strength**
 - Higher contact force gives larger pull-off force
 - Slower retraction causes larger pull-off force
- Pull-off force measurements, normal & horizontal dynamics: **Weak Bond Strength**
 - Faster horizontal motion (micron range) yields lower pull-off force

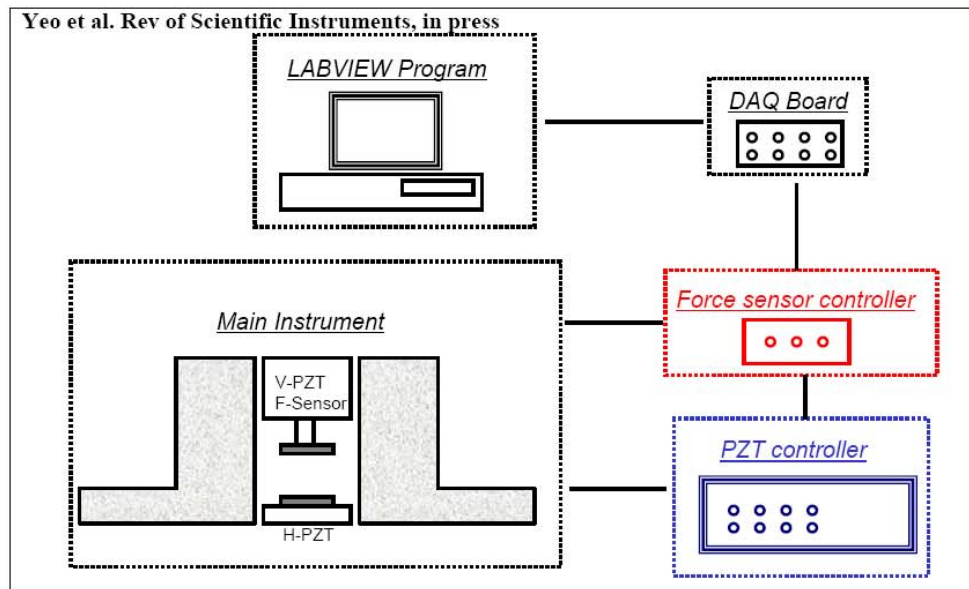


University of Illinois at Urbana-Champaign



5

4. Instrumentation: Schematic

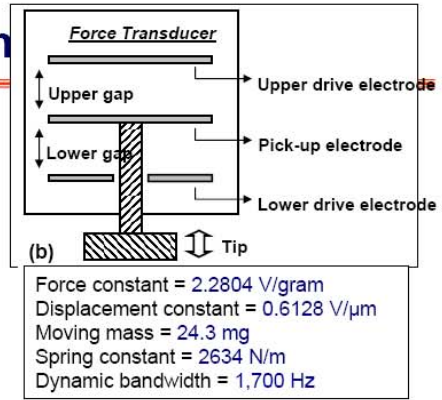
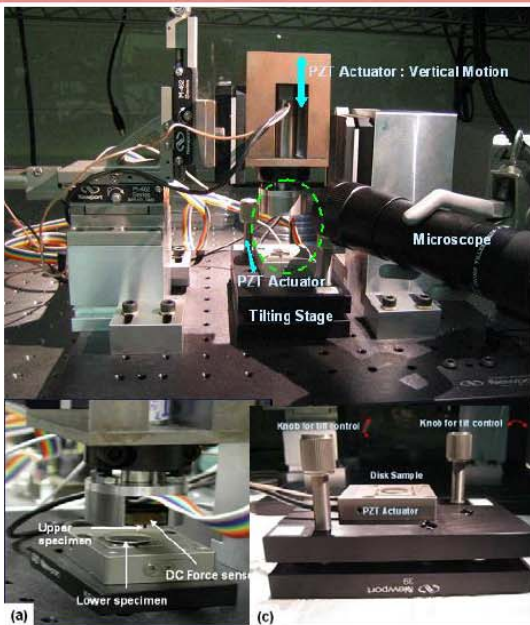


University of Illinois at Urbana-Champaign



6

4. Actual Instrumentation



- Vertical approaching/retracting velocity: By PZT actuator (ref. **VPZT**)
- Horizontal bi-directional velocity: By PZT actuator (ref. **HPZT**)
- Force sensor + DAQ board + Labview: Interfacial force measurements

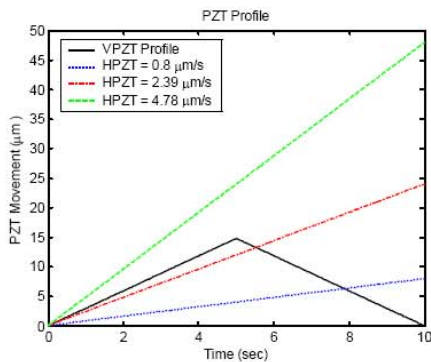
University of Illinois at Urbana-Champaign



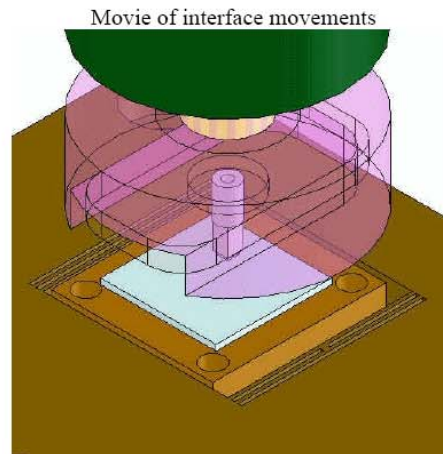
7

4. Motion Profile 1

VPZT = Vertical PZT motion (top sample)
 HPZT = Horizontal PZT motion (bottom sample)



- Bottom surface
- 1-way motion during tip approaching/retracting



The movie is on "self-play" in slide show mode

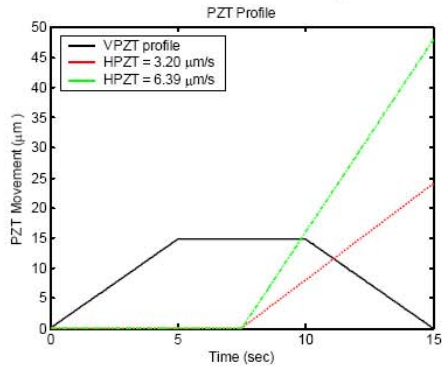
University of Illinois at Urbana-Champaign



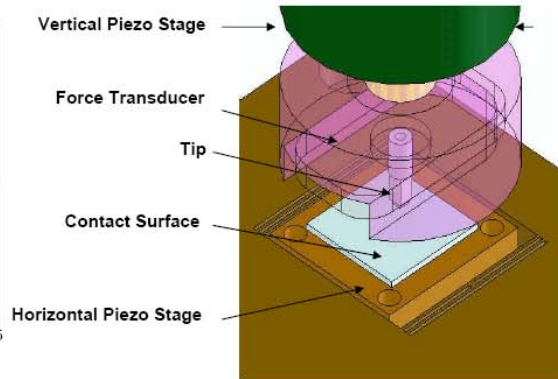
8

4. Motion Profile 2

VPZT = Vertical PZT motion (top sample)
 HPZT = Horizontal PZT motion (bottom sample)



Movie of interface movements

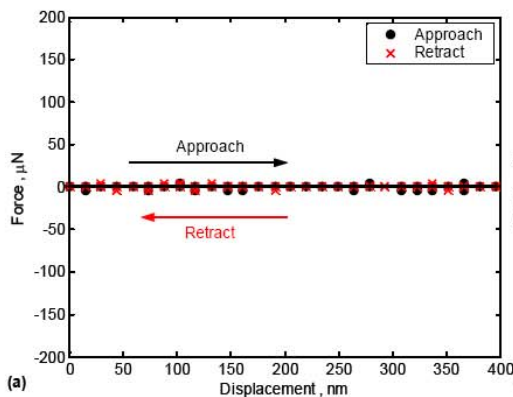


- Bottom surface
 - 1-way motion in the middle of contact

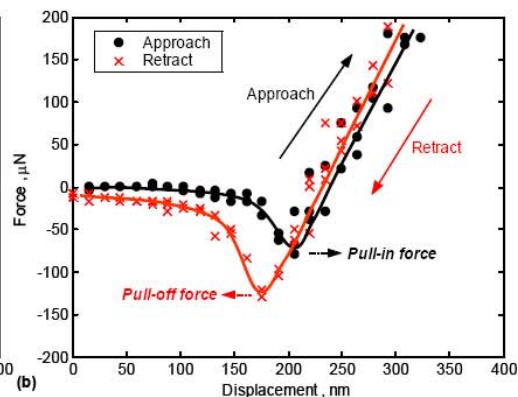
The movie is on "self-play"
 in slide show mode

4. Typical Dynamic Adhesive Force Measurements

- No interactive forces
 - "far away" from the contacting surface



- Clear interactive forces
 - near the contacting surface



- No inertia effects
- $\pm 1.7 \mu\text{N}$ RMS force resolution

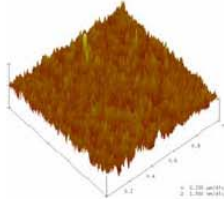
- Approach: Pull-in force
- Retract: Pull-off force

5. Samples: “Meso scale” samples

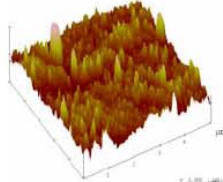
A. Spherical samples

(1) Al₂O₃/TiC sphere (1 mm radius)

(2) Stainless steel sphere (0.794 mm radius)



RMS roughness = 25.8 nm



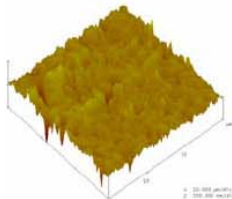
RMS roughness = 5.25 nm

B. Flat samples

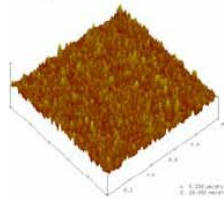
(1) Silicon wafer <100>

(2) 10 nm carbon film on glass substrate

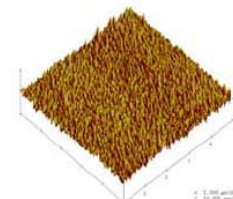
(3) Au(1 μm) sputtered on Silicon wafer substrate



RMS roughness = 0.11 nm



RMS roughness = 0.77 nm



RMS roughness = 3.84 nm

University of Illinois at Urbana-Champaign



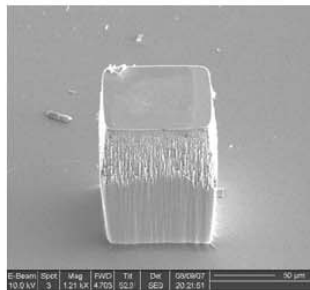
11

5. Samples: “Micro scale” samples

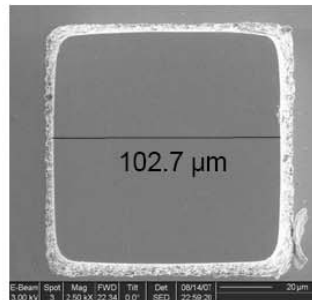
C. Custom-fabricated pattern surfaces: Silicon <100>

(1) Pillar with plane top surface

(2) Pillar with grooved top surface
Pitch 400 nm, depth 100 nm (FIB)



RMS roughness = 1.09 nm

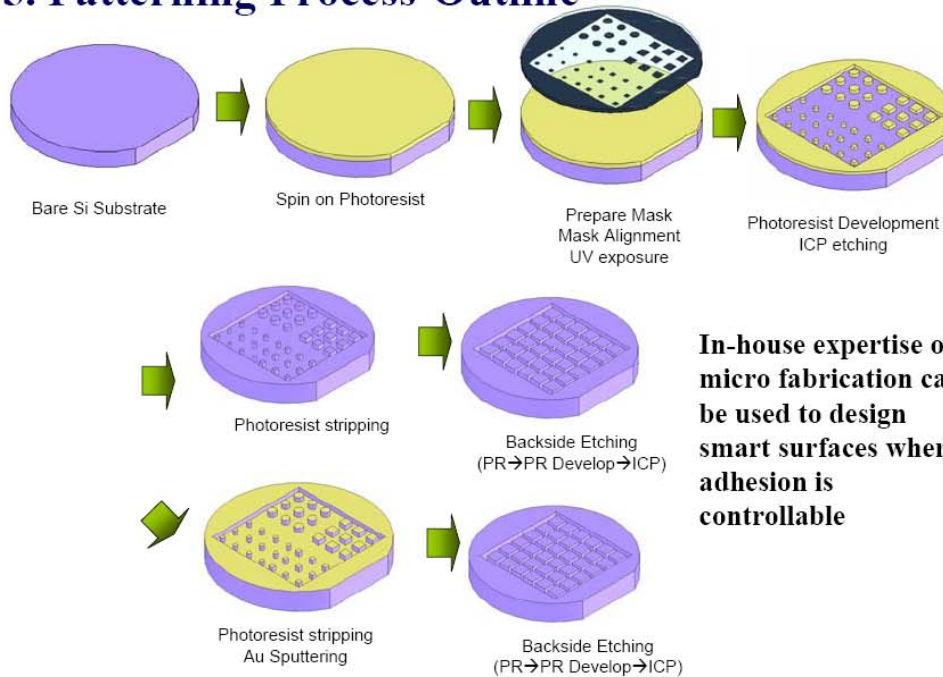


University of Illinois at Urbana-Champaign



12

5. Patterning Process-Outline



6.1 Experiments: Vertical Dynamics

□ Testing conditions

- Upper specimen: $\text{Al}_2\text{O}_3/\text{TiC}$ sphere (1 mm radius)

Velocity change in z-direction

- Lower specimen: 10 nm COC Disk sample

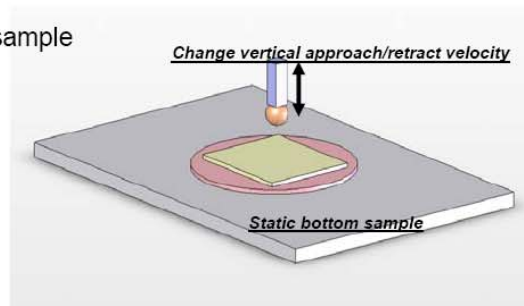
Static

- Test Conditions

- Contact Force level
- $70 \mu\text{N}$ / $220 \mu\text{N}$ / $770 \mu\text{N}$

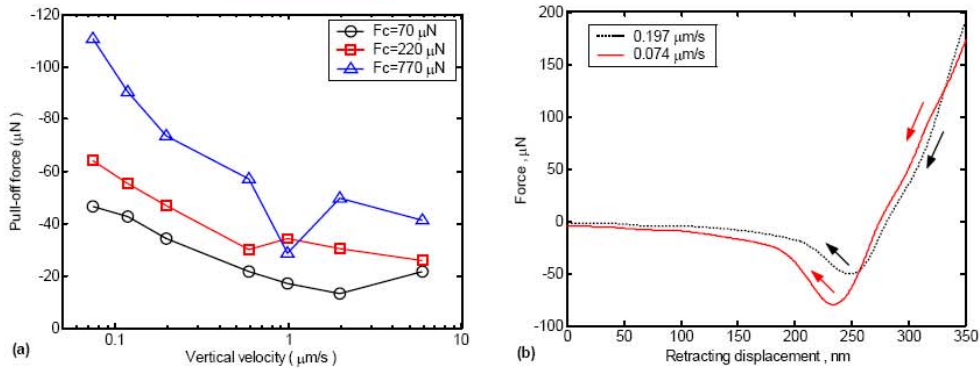
- Velocity level in z-direction

Velocity 1	Velocity 2	Velocity 3	Velocity 4	Velocity 5	Velocity 6	Velocity 7
5.922	1.974	0.987	0.592	0.198	0.118	0.074



6.1 Experiments: Vertical dynamics

□ Pull-off [De bonding] forces vs. Vertical velocity



➤ Pull-off (de bonding) force vs. Velocity Observations:

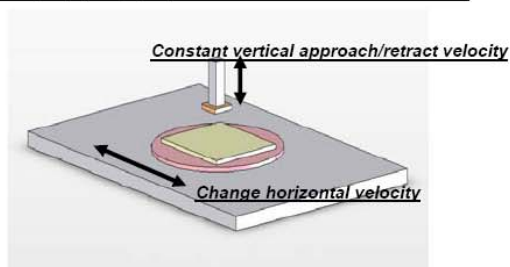
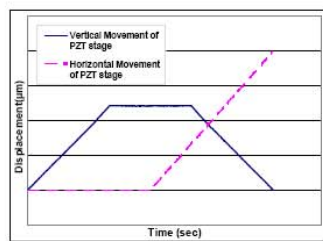
- Higher contact force causes larger pull-off force
- Slower velocity causes later jump-out behavior with larger pull-off force
- For a stronger solid bond: Higher contact force and slower velocity
- For de bonding (weak bond): Fast retracting velocity

6.2 Experiments: Horizontal Dynamics

□ Interactive adhesive forces w.r.t. horizontal velocity changes

□ Testing conditions

	Upper Tip	Bottom surface
1	Silicon (1mmx1mm)	Silicon (1mmx1mm)
2	Steel ball (R=0.794 mm)	PSA
3	Au(1 μm) coated on Silicon (1mmx1mm)	Au(1 μm) coated on Si
4	Steel ball (R=0.794 mm)	Photoresist(8 μm) coated on Silicon
5	Au(1 μm) coated on Silicon (200 μm x 200 μm)	Au(1 μm) coated on Si



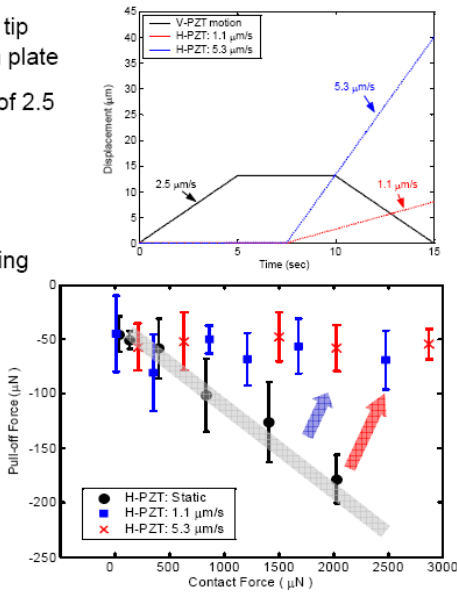
6.2 Experiments: Horizontal Dynamics

□ Specimen

- Squared Silicon {100} (1 mm²) on upper tip
- Squared Silicon {100} (1 cm²) on bottom plate
- Upper specimen: Constant vertical velocity of 2.5 μm/s
- Lower specimen: 1-way movement (8 μm)
- starting at the middle of the contact
- Pull-in and Pull-off force measurements during horizontal movement of the bottom surface

□ Observations

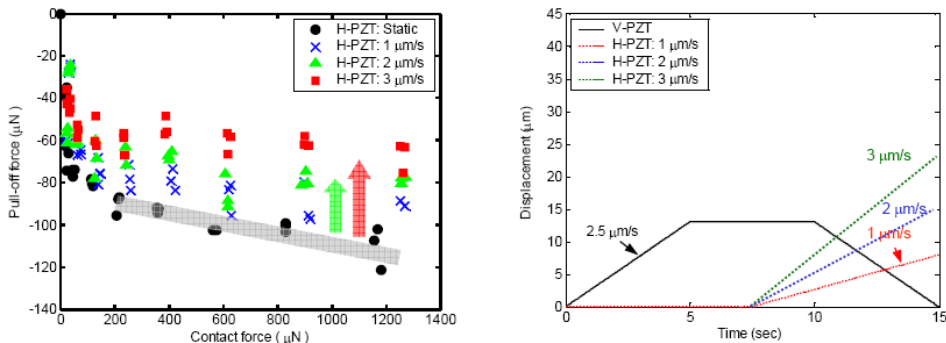
- Under static bottom sample conditions, larger contact force gives higher pull-off forces [Strong Bond]
- Once the bottom sample moves horizontally, the pull-off force dramatically decreases [Weaker De bond]



6.2 Experiments: Horizontal Dynamics

□ Specimen

- Steel ball ($R = 0.794$ mm) on upper tip
- Uniform tacky silicon pressure sensitive adhesive (1 cm × 1 cm) on bottom

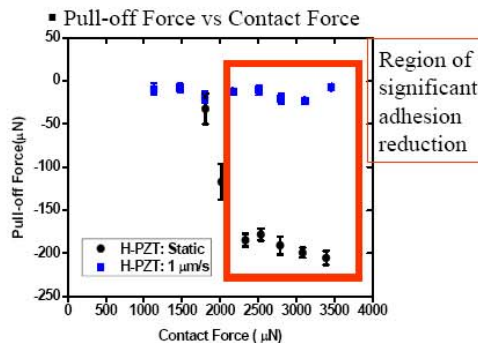
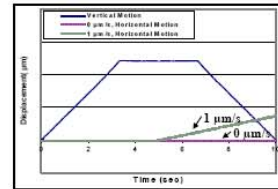


- Once the bottom sample moves horizontally, the pull-off force decreases
- The faster horizontal motion gives lower pull-off forces
- Note that the decrease in bond strength is small because the horizontal motion was only few microns, thus unable to break all the interface bonds

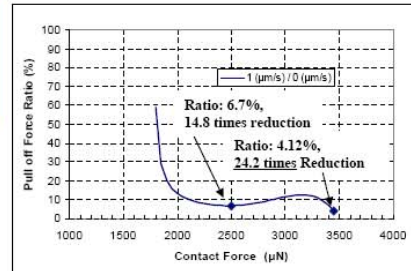
6.2 Experiments: Horizontal dynamics

□ Testing conditions

- Au coated silicon wafer sample (1 mm x 1 mm) on upper tip
- Au coated silicon wafer sample on bottom surface
- Contact Pressure: 3 kPa (at 3000 μN)
- Humidity level: 55%; Temp:24.5°C



▪ Pull-off Force Ratio

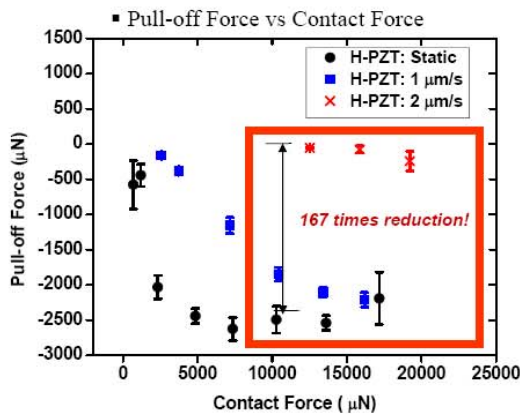


- There is a clear reduction of adhesion (pull-off force) or bond strength when imposing a small horizontal movement at the interface. It is of the order of more than an order of magnitude

6.2 Experiments: Horizontal dynamics

□ Testing conditions

- Steel ball ($R=1.6$ mm) on upper tip
- Photoresist ($8 \mu\text{m}$) coated on silicon wafer on the bottom surface



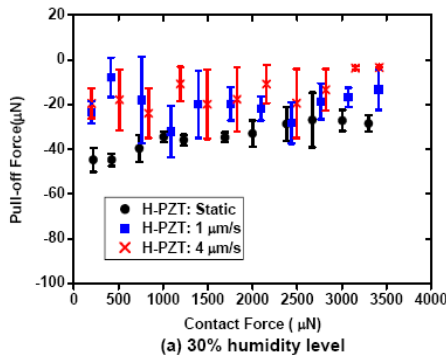
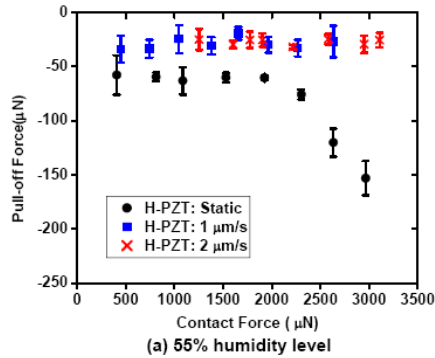
- Thin sticky coating layer of PR works effectively
- Works in high contact pressure: 28.74 MPa ~ 54.37 MPa (@ 13000 μN)
- Note that the Modulus of Elasticity varies from 1 GPa to 4 GPa for a PR that has not been fully baked.
- Very large reduction of adhesion is seen. (167 times @ 13000 μN)

6.2 Experiments: Horizontal dynamics

□ Testing conditions

- Au coated silicon wafer sample (200 μm x 200 μm) on upper tip
- Au coated silicon wafer sample on bottom surface

• Contact Pressure: 12.5 kPa ~ 75 kPa (500 μN ~ 3000 μN)



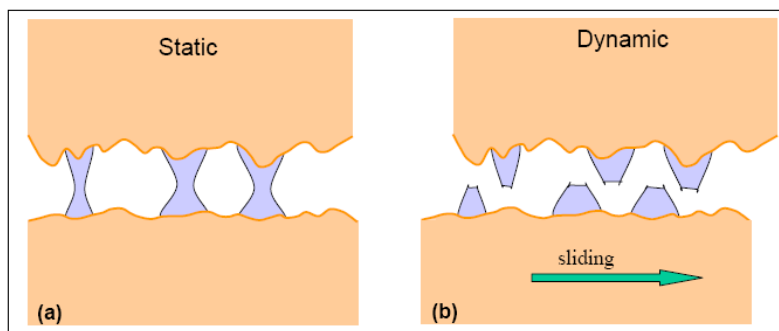
- Overall trend is similar to the previous tests.
- Difference of humidity level results in different adhesion and pull-off forces

6.3 Physical Explanation

Static contact: Asperity junctions made of material adhesion or liquid column (meniscus)

Breakage of the asperity junctions

Dramatic reduction of adhesive forces → Detach the contacting surface



7. Summary

Adhesive forces under vertical dynamic motion only

- For stronger solid bond: Higher contact force and slower velocity (also other effects such as increased area and different materials could be investigated)
- For de bonding (weak bond): Fast retracting velocity

Adhesive forces under vertical and horizontal motions

- Once we have a strong bond (static condition), the faster the horizontal motion at the interface the lower the debonding force
- According to the properties of contacting surfaces, adhesion and pull-off forces vary significantly
- Gold coated samples (area of 1mm²) under a contact force of 3000 μ N, the adhesion force was 24.2 times greater than that of the pull-off force, where the photoresist coated sample gave a ratio of 167

This study provides a proof of concept that using proper material selection and interfacing surfaces, the adhesion force can be maximized and can be minimized with the proper aid of shearing force.

8. Future Work

- Proof-of-concept accomplished (strong Vs weak bonding of solid surfaces)
- Specifically design surfaces and surface features to have variable bond strengths: it can be accomplished, for example, with microfabricated features on surfaces that can move in the normal and/or horizontal directions, thus turning adhesion on and off, as desired
- Such surfaces will need to be optimized to work under different environments (liquid, dry, sandy etc)